Doppler optical microangiography improves the quantification of local fluid flow and shear stress within 3-D porous constructs

Yali Jia, Lin An, and Ruikang K. Wang*
Oregon Health & Science University, Department of Biomedical Engineering, 3303 South West Bond Avenue, Portland, Oregon 97239

Abstract. Traditional phase-resolved Doppler optical coherence tomography (DOCT) has been reported to have potential for characterizing local fluid flow within a microporous scaffold. In this work, we apply Doppler optical microangiography (DOMAG), a new imaging technique developed by combining optical microangiography (OMAG) with a phase-resolved method, for improved assessment of local fluid flow and its derived parameters, shear stress, and interconnectivity, within highly scattering porous constructs. Compared with DOCT, we demonstrate a dramatic improvement of DOMAG in quantifying flow-related properties within scaffolds *in situ* for functional tissue engineering. [DOI: 10.1117/1.3233590]

Keywords: tissue engineering; porous scaffold; fluid flow; shear stress; optical coherence tomography; optical microangiography.

Paper 09237LR received Jun. 9, 2009; revised manuscript received Jul. 23, 2009; accepted for publication Jul. 25, 2009; published online Oct. 7, 2009.

The aim of functional tissue engineering (FTE) is to grow a complete 3-D biotissue coupled with appropriate, biological functionalities for implanting into the body, with the purpose of fostering remodeling and regeneration of diseased tissue.[1] To provide a suitable template to support cell growth and to deliver sufficient amounts of nutrients during tissue development, a 3-D porous scaffold is one critical ingredient involved in FTE. Its architectural properties, pore interconnectivity for example, largely determine the interactions among groups of cells, which facilitate cell-cell communications and tissue integrity.[2] A bioreactor is another key element in FTE, providing the necessary physical regulatory environment to guide appropriate cell differentiation and tissue development. Mechanical stimulus such as fluid-induced shear stress has a well-known impact on cell morphology and orientation, and is also an important modulator of cell physiology. There is considerable evidence that mechanical stress affects gene expression, and subsequently protein synthesis, cell proliferation, and differentiation,[3,4] and significantly increases the biosynthetic activity in a range of different cell types.[5,6] *In vitro* studies have shown that mechanical stress in culture environments, such as within bioreactors, presents biphasic dose-response characteristics. This suggests that excessive stress force that produces cell distortion may also play a role to switch cells between motility and apoptosis programming.[7] To further understand the mechanisms of dynamic interaction between the cell growing behavior and the mechanical shear stress, a nondestructive imaging technique is needed capable of imaging the localized fluid flow and shear stress *in situ* within the entire porous scaffold (with a typical thickness of approximate millimeters), preferably at a level of the individual micropores. However, such requirements of monitoring and imaging in tissue engineering is difficult, if not impossible, to fulfill by use of current imaging technologies.

Recently, phase-resolved Doppler optical coherence tomography (DOCT) has been reported to have potential to image local fluid flow, and subsequently to characterize shear stress and pore interconnectivity in 3-D porous scaffolds.[8] Although promising, the performance of DOCT is severely limited by a background texture noise presented in the system, imposed by the optical heterogeneous property of the tissue sample.[9] Most recently, a novel imaging method, Doppler optical microangiography (DOMAG), is reported to evaluate the velocities of blood flow within microcirculatory tissue beds with much improved precision.[10] Combined with the phase-resolved method developed in DOCT, DOMAG extracts flow velocities from OMAG flow signals. In this work, we briefly discuss how DOMAG improves imaging fidelity of fluid flow by use of a flow phantom, and then we report the utility of DOMAG to explore fluid flow, shear stress, and interconnectivity within 3-D porous scaffolds with an unprecedented accuracy as compared to DOCT.

The configuration and operating principles of the DOMAG system can be found elsewhere.[10] Briefly, the system used in this study employed a broadband infrared superluminescent diode with a central wavelength of 1300 nm. The spectral interferogram formed by lights between the sample and reference arms was sent to a home-built high-speed spectrometer that employed a line scan infrared InGaAs detector to achieve an imaging speed of 20 frames per second (fps) with 1000 A scans (axial scans) in each B scan (lateral direction). The system has the imaging resolution of $16\times16\times8$ μm^3 in the x-y-z direction, and an imaging depth of ~3 mm in air.

To test DOMAG performance in imaging flow, we first used DOMAG to image a flow phantom. The phantom was made from gelatin mixed with 2% milk to simulate the heterogeneous tissue background, within which a capillary tube with an inner diameter of ~200 μm was submerged, and ~2% TiO_2 particle solution was flowing in it. The Doppler angle was set at 85 deg. The flow rate was controlled by a precision syringe pump. Figure 1(a) shows a crosssectional OMAG structural image of the scanned flow phantom that is identical to the image obtained by frequency domain optical coherence tomography (FDOCT). The phase difference result in Fig. 1(b) is described by conventional DOCT to represent the flow velocity information. Due to the optical heterogeneity of a static tissue background [denoted by B_t in Fig. 1(a)], a background noise [N_b in Fig. 1(b)] from the nonflow region of the phantom was imposed onto the DOCT flow image, making it difficult for DOCT to precisely measure small flow velocity.[11] An additional problem in DOCT is the random noise [labeled

*Tel: 503-748-1350; E-mail: wangr@ohsu.edu or r.k.wang@bme.ogi.edu

1083-3668/2009/14(5)/050504/3/$25.00 © 2009 SPIE

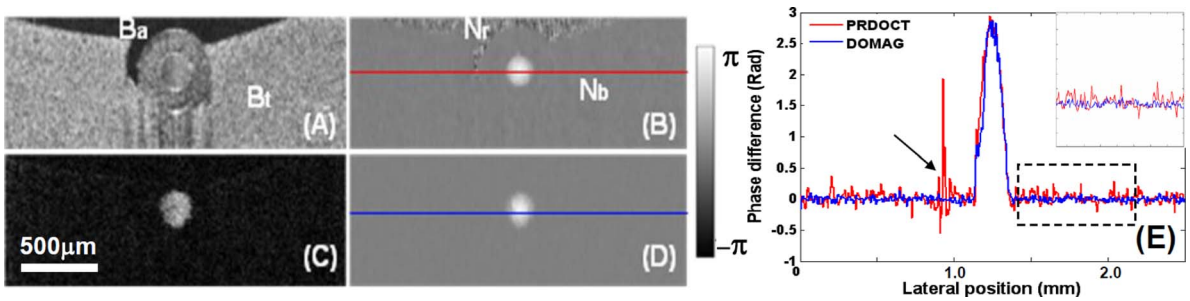

Fig. 1 Typical cross-sectional images of the flow characteristics in a flow phantom. (a) OMAG structural image. Ba = background of air; Bt = background of tissue. (b) DOCT velocity image. Nr = random noise; Nb = background noise. (c) OMAG flow image. (d) DOMAG velocity image. (e) Flow signal profiles extracted from the positions marked in (b) and (d), where the insert is the enlargement of the marked area. The black arrow indicates the area over which the random noise is generated.

with N_r in Fig. 1(b)] from the background with low backscattered signal, such as the air region in this phantom [labeled with B_a in Fig. 1(a)]. Before evaluating flow signals, the segmentation method has to be used to extract the tissue regions of interest. These two types of artifacts from backgrounds are maximally suppressed with the advent of the DOMAG imaging method. Figure 1(c) shows the corresponding OMAG flow, image that delineates the scattering fluid flow, with both background noise and random noise being rejected. The OMAG method successfully separated the backscattering flow signals from the background signals, resulting in minimal noise production.[10,12] When combined with the phase resolved method, it is clear that DOMAG in Fig. 1(d) provides superior imaging performance due to noise suppression in either tissue or air background when compared to Fig. 1(b). To better show the noise suppression by DOMAG, we extracted two signal profiles across the same depth position marked by red and blue lines in Figs. 1(b) and 1(d), respectively. The corresponding signal profiles are shown in Fig. 1(e). The phase differences (parabolic curve) in the flow region are almost the same by different methods, but the background noise in DOMAG (~0.02 rad) is much smaller than that in DOCT (~0.15 rad), and the random noise in DOCT (indicated by the black arrow) was removed in DOMAG due to its reconstruction procedure. Consequently, we expect that the phase SNR will increase in DOMAG as compared to DOCT, delivering improved evaluation of fluid flow and shear stress.

Next, we applied DOMAG in noninvasive assessment of fluid flow through porous microstructures in chitosan scaffolds, widely used in FTE. Chitosan scaffolds with high porosity were fabricated as described in Ref. 8, then placed within a transparent sample chamber (ID=1.5 mm) for DOMAG imaging. During imaging, the chamber was oriented to have a Doppler angle of 85 deg with respect to the incident probe beam. A precision syringe pump was used to deliver a constant input flow rate of 8 ml/h. A 0.5% latex microsphere (0.3 μm in diameter) suspension was used as the light scattering medium. Shown in Fig. 2 are the representative results from a single B scan of the scaffold. Figure 2(a) is the OMAG structural image taken before scattering medium flowed through the sample, from which the microstructures of the pores are clearly delineated. Figure 2(b) shows the corresponding OMAG image of localized fluid flow that permeates this cross section shown in Fig. 2(a). However, this image only provides the backscattered signals (i.e., reflectance) from the functional flow that does not indicate the flow velocity information, which is, however, needed for quantifying the localized shear stress. By applying the DOMAG method, the phase difference map [Fig. 2(c)] to the imaged fluid flow was extracted from Fig. 2(b), which could then be converted to the velocity values. Compared with the result from the same section obtained by DOCT [Fig. 2(d)], the fluid flow with relative small velocities corresponding to the small values of phase difference[12] can be successfully captured by DOMAG [Fig. 2(c)]. As discussed in our previous work, in DOCT, background phase noise is a barrier to imaging the detailed velocities of flow due to the heterogeneity of the scaffold, as seen in Fig. 2(d). When the scan rate was set at 20 kHz, the noise floor in DOCT was typically 0.4 rad for the scaffold studied, suggesting that DOCT might fail to measure flow <0.83 mm/s. Therefore, slow flows (<0.83 mm/s) in the microstructures were masked due to the noise production in DOCT. DOMAG is capable of reducing this noise level to 0.03 rad, which corresponds to the minimal detectable velocity of ~62 μm/s. As a consequence, the low fluid flow near the wall of micropores (>62 μm/s) is detected by DOMAG. This advantage makes DOMAG a more powerful tool in imaging fluid flow in the cultured, complex microconstructs that are usually perfused by a low input flow rate.

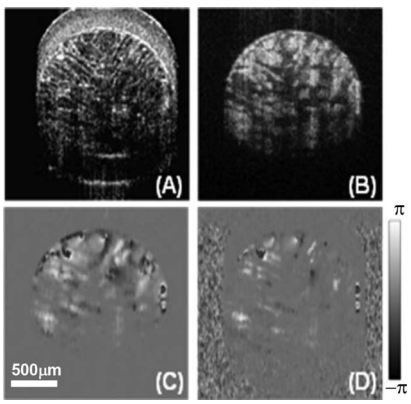

Fig. 2 *In situ* imaging results for a typical B scan of the porous scaffolds. (a) OMAG structural image taken before scattering medium flowed through the sample. And OMAG images of (b) fluid flows and (c) their velocities respectively. (d) corresponding DOCT image of fluid flow.

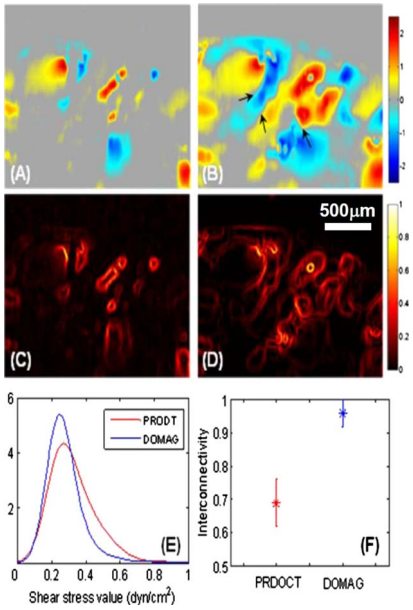

Fig. 3 *In situ* assessment of shear stress and interconnectivity in porous scaffold via DOMAG and DOCT, respectively. Shown are (a) DOCT and (b) DOMAG images of velocities of fluid flow, respectively; and the corresponding (c) DOCT and (d) DOMAG image of local shear stress distributions. (e) is wall shear stress distribution (n=12), and (f) the interconnectivity (mean ± std) (n=12). Color bar units = mm/s (upper row), and dyn/cm^2 (middle row). (Color online only.)

Lastly, we provide a comparison between these two techniques for measuring shear stress and interconnectivity through the use of the same dataset scanned from a perfused scaffold. Figures 3(a) and 3(b) show the directional phase difference maps generated by DOCT and DOMAG, respectively. It is noted that we have to reduce the noise artifacts in the DOCT flow image to evaluate shear stress and pore interconnectivity. As the noise level of DOMAG is low in the entire image, noise reduction is not required. Compared to the DOCT image in Fig. 3(a), Fig. 3(b) shows that DOMAG detects the fluid flow within almost all micropores in the scanned construct, and more importantly, it illustrates that the slow flows near the pore walls (e.g., indicated by black arrows) are detected by DOMAG that are not visible by DOCT. The ability of DOMAG to image the flows near the wall is important because they are critical to deduce the localized shear stresses.[8] These results indicate that DOMAG promises a nondestructive imaging technique to reliably determine the localized shear stress values within porous structures. The corresponding shear stresses are shown in Figs. 3(c) and 3(d), respectively. It can be seen that most values are distributed on the pore walls in Fig. 3(d), because slower flows emerging along walls were detected by the DOMAG method. However, higher values were derived by DOCT [Fig. 3(c)] due to the high noise floor that had to be removed before calculating the shear stress values, leading to an overestimate of the localized shear stress. As a consequence, DOMAG is capable of more precisely detecting the shear stress distribution in perfused constructs. In Fig. 3(e), the probability of shear stress value shown by probability mass function (n=12) is compared between DOCT and DOMAG. Visually, the shear stresses via DOMAG were distributed less broadly than those via DOCT, indicating that detectable shear stress became more uniform in DOMAG, which caused the mean shear stress to decrease. Furthermore, the pore-interconnectivity evaluation from the flow image maps from two methods are presented in Fig. 3(f) (n=12). The mean value of DMOAG is ~1.5-fold larger than that of DOCT, suggesting the advantage of DOMAG over DOCT in quantifying how much space is being used for transfusion in the artificial tissues.

In summary, we have successfully demonstrated the use of DOMAG for improved characterization of local fluid flow within highly scattering microporous scaffolds *in situ*. By rejecting the background noise imposed by the heterogeneous properties of tissue samples, OMAG is able to detect the slow fluid flow near the porous wall within the microporous tissue constructs. The improved assessment of shear stress and interconnectivity values based on the flow information shows promise for DOMAG to monitor the dynamic properties of an engineered tissue in a bioreactor.

Acknowledgment

The authors would like to thank Pierre Bagnaninchi (Edinburgh University, United Kingdom) in assisting with the preparation of porous chitosan scaffolds used in this study. The work was supported in part by research grants from the National Institutes of Health (R01 HL093140, R01 EB009682, and R01 DC010201), and the American Heart Association (0855733 G).

References

1. R. Langer and J. P. Vacanti, "Tissue engineering," *Science* **260**, 920–926 (1993).
2. R. C. Thomson, A. G. Mikos, E. Beahm, J. C. Lemon, W. C. Satterfield, T. B. Aufdemorte, and M. J. Miller, "Guided tissue fabrication from periosteum using preformed biodegradable polymer scaffolds," *Biomaterials* **20**, 2007–2018 (1999).
3. B. O. Oluwole, W. Du, I. Mills, and B. E. Sumpio, "Gene regulation by mechanical forces," *Endothelium* **5**, 85–93 (1997).
4. D. P. Bottaro, A. Liebmann-Vinson, and M. A. Heidaran, "Molecular signaling in bioengineered tissue microenvironments," *Ann. N.Y. Acad. Sci.* **961**, 143–153 (2002).
5. T. Davisson, R. L. Sah, and A. Ratcliffe, "Perfusion increases cell content and matrix synthesis in chondrocyte three-dimensional cultures," *Tissue Eng.* **8**, 807–816 (2002).
6. G. N. Bancroft, V. I. Sikavitsas, J. van den Dolder, T. L. Sheffield, C. G. Ambrose, J. A. Jansen, and A. G. Mikos, "Fluid flow increases mineralized matrix deposition in 3D perfusion culture of marrow stromal osteoblasts in a dose-dependent manner," *Proc. Natl. Acad. Sci. U.S.A.* **99**, 12600–12605 (2002).
7. S. H. Cartmell, B. D. Porter, A. J. Garcia, and R. E. Guldberg, "Effects of medium perfusion rate on cell-seeded three-dimensional bone constructs *in vitro*," *Tissue Eng.* **9**, 1197–1203 (2003).
8. Y. L. Jia, P. O. Bagnaninchi, Y. Yang, A. J. El Haj, M. T. Hinds, S J. Kirkpatrick, and R. K. Wang, "Doppler optical coherence tomography imaging of local fluid flow and shear stress within microporous scaffolds," *J. Biomed. Opt.* **14**, 034014 (2009).
9. R. K. Wang and Z. H. Ma, "Real-time flow imaging by removing texture pattern artifacts in spectral-domain optical Doppler tomography," *Opt. Lett.* **31**, 3001–3003 (2006).
10. R. K. Wang and L. An, "Doppler optical micro-angiography for volumetric imaging of vascular perfusion *in vivo*," *Opt. Express* **17**, 8926–8940 (2009).
11. R. K. Wang, S. L. Jacques, Z. Ma, S. Hurst, S. R. Hanson, and A. Gruber, "Three dimensional optical angiography," *Opt. Express* **15**, 4083–4097 (2007).
12. Z. P. Chen, T. E. Milner, S. Srinivas, X. Wang, A. Malekafzali, M. J. C. van Gemert, and J. S. Nelson,"Noninvasive imaging of *in vivo* blood flow velocity using optical Doppler tomography," *Opt. Lett.* **22**, 1119–1121 (1997).